A&A 489, 1023–1028 (2008)
DOI: 10.1051/0004-6361:200810166

Astronomy & Astrophysics

Compact stellar systems in the Fornax cluster: a UV perspective⋆ *(Research Note)*

S. Mieske[1], M. Hilker[1], D. J. Bomans[2], S.-C. Rey[3], S. Kim[3], S.-J. Yoon[4], and C. Chung[4]

[1] European Southern Observatory, Karl-Schwarzschild-Strasse 2, 85748 Garching bei München, Germany
e-mail: smieske@eso.org
[2] Astronomical Institute, Ruhr-University Bochum, Universitätsstr. 150, 44780 Bochum, Germany
[3] Department of Astronomy and Space Science, Chungnam National University, Daejeon 305-764, Korea
[4] Department of Astronomy & Center for Space Astrophysics, Yonsei University, Korea

Received 9 May 2008 / Accepted 8 July 2008

ABSTRACT

Context. There is increasing evidence for chemical complexity and multiple stellar populations in massive globular clusters (GCs), including extreme horizontal branches (EHBs) and UV excess.
Aims. We aim to improve our understanding of the UV excess in compact stellar systems, covering the regime of both ultra-compact dwarf galaxies (UCDs) and massive GCs.
Methods. We use deep archival GALEX data of the central Fornax cluster to measure *NUV* and *FUV* magnitudes of UCDs and massive GCs.
Results. We obtain *NUV* photometry for a sample of 35 compact objects that cover a range $-13.5 < M_V < -10$ mag. Of those, 21 objects also have *FUV* photometry. Roughly half of the sources fall into the UCD luminosity regime ($M_V \lesssim -11$ mag). We find that seven out of 17 massive Fornax GCs exhibit a *NUV* excess with respect to expectations from stellar population models, both for models with canonical and enhanced Helium abundance. This suggests that not only He-enrichment has contributed to forming the EHB population of these GCs. The GCs extend to stronger UV excess than GCs in M 31 and massive GCs in M 87, at the 97% confidence level. Most of the UCDs with *FUV* photometry also show evidence for UV excess, but their UV colours can be matched by isochrones with enhanced Helium abundances and old ages 12–14 Gyr. We find that Fornax compact objects with X-ray emission detected from Chandra images are almost disjunct in colour from compact objects with GALEX UV detection, with only one X-ray source among the 35 compact objects. However, since this source is one of the three most UV bright GCs, we cannot exclude that the physical processes causing X-ray emission also contribute to some of the observed UV excess.

Key words. galaxies: clusters: individual: Fornax – galaxies: dwarf – stars: horizontal-branch – stars: evolution – galaxies: star clusters

1. Introduction

Evidence of chemical complexity and multiple stellar populations has been found in several massive Galactic globular clusters (GCs) (e.g. Gratton et al. 2004; Bedin et al. 2004; Piotto et al. 2007; Milone et al. 2008). For some globular clusters (e.g. ω Centauri and NGC 2808), there is evidence that these multiple populations may be due to an enhancement in Helium content (up to $Y \simeq 0.4$), as deduced from the presence of extremely blue horizontal branches (EHBs) and multiple main sequences (D'Antona et al. 2005; Lee et al. 2005). The link between the presence of EHBs and He-enhancement is, however, under debate. EHB stars may also originate directly from fast rotating stars with an enhanced mass loss during the red giant branch (RGB) evolution. Those stars leave the RGB before the He flash towards the (He-core) white dwarf cooling curve where they ignite Helium and end up on the EHB (Castellani & Castellani 1993; D'Cruz et al. 1996; Brown et al. 2001). This is sometimes referred to as the "hot-flasher" scenario. A significant fraction of EHB stars in ω Centauri appear to have followed this evolutionary path (Moehler et al. 2007).

It has been shown that EHB stars contribute to most of the light in the UV bands (e.g. NGC 2808; Dieball et al. 2005). The presence of an EHB in extragalactic – unresolved – GCs is inferred from a UV-excess in the integrated light compared to GCs with a "normal" horizontal branch (HB). Rey et al. (2007) found three metal-rich ([Fe/H] > -1) GC candidates in M 31 with significant *FUV* flux, which were interpreted as analogs of two peculiar Galactic GCs, NGC 6388 and NGC 6441 (Yoon et al. 2008). Sohn et al. (2006) and Kaviraj et al. (2007) analysed the UV properties of massive globular clusters associated with M 87 in the Virgo cluster, and found that many had a UV-excess with respect to canonical stellar population models. These findings support the idea that EHBs may be a common feature in the most massive compact stellar systems.

In this Research Note, we focus on the UV properties of compact stellar systems in the Fornax cluster. In contrast to the studies of Sohn et al. and Kaviraj et al. of Virgo GCs, we extend our analysis to compact stellar systems beyond the mass range of GCs ($M \lesssim 3 \times 10^6\ M_\odot$), including the so-called ultra-compact dwarf galaxies (UCDs, Drinkwater et al. 2003), which have masses up to $\sim 10^8\ M_\odot$, and $M_V \lesssim -11$ mag. We compare the UV properties of UCDs to those of both massive and normal GCs, in order to improve our knowledge of the incidence of EHBs in compact stellar systems. Throughout this study, we

⋆ Based on observations made with the NASA Galaxy Evolution Explorer GALEX. GALEX is operated for NASA by the Califonia Institute of Technology under NASA contract NAS5-98034.

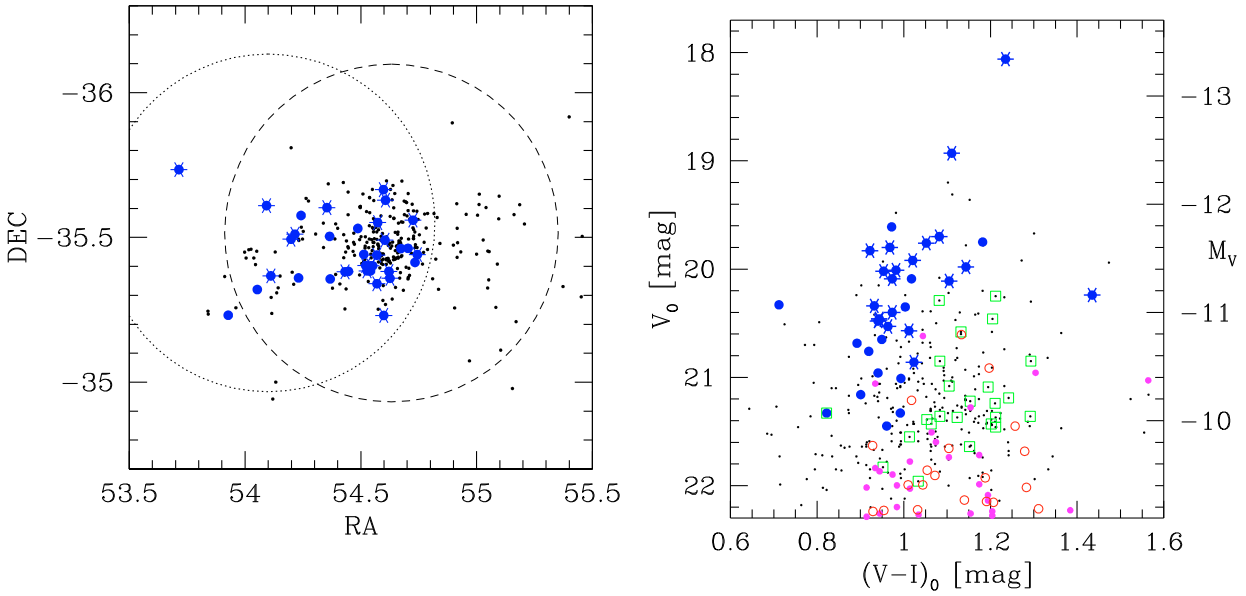

Fig. 1. *Left*: map of the central Fornax cluster. The large circles indicate the FoV of the two archival GALEX pointings used for this study. The large dotted circle corresponds to the Deep Imaging Survey (DIS), the large dashed circle corresponds to the Near Galaxies Survey (NGS). The small dots indicate our sample of spectroscopically confirmed compact objects down to $V \simeq 22$ mag ($M_V = -9.4$ mag). The filled circles indicate the sources with visually verified GALEX matches in the *NUV*, where the asterisks are those sources with matches in the *FUV* (matching radius 3″). *Right*: V, I colour–magnitude diagram of the same sources as in the *left panel*. The optical data is from Mieske et al. (2004, 2006, 2007), and Dirsch et al. (2003). Green squares indicate sources with X-ray counterparts from the Chandra study of Scharf et al. (2005). Magenta dots indicate GCs in M 31 with UV colours available (Fig. 2; Rey et al. 2007), red circles indicate GCs in M 87 with *FUV* colours available (Fig. 2; Sohn et al. 2006). Note that only one of the GALEX UV detections has a detected X-ray counterpart.

adopt $(m-M) = 31.4$ mag (Freedman et al. 2001) as the distance modulus of the Fornax cluster.

2. The data

To investigate the UV properties of massive compact stellar systems in Fornax, we retrieved archival *FUV* and *NUV* GALEX images from two pointings in the Fornax cluster[1]. One pointing was offset from NGC 1399 by about 0.4° to the west, and was aquired as part of the Deep Imaging Survey (DIS) with integration time 18 000 s. The other pointing was centred on NGC 1399, taken within the Near Galaxy Survey (NGS), of integration time 1700 s in *FUV* and *NUV* (see Fig. 1).

We subtracted models of the two giant elliptical galaxies NGC 1399 and NGC 1404 from the archival GALEX images, using the modelling routines `ellipse` and `bmodel` within IRAF. We then executed SExtractor on the images to create a source catalog of detections in *NUV* and *FUV*. For this, we required a minimum of 5 adjacent pixels with fluxes at least 2σ above the sky noise. We adopted MAG_BEST as the source magnitude, and used the GALEX photometric zero-points given in the image headers. From artificial star experiments using the same detection parameters, we derived 50% completeness limits for unresolved sources in the DIS images of $NUV_0 = 24.2$ mag and $FUV_0 = 24.7$ mag. The region within $\simeq 2'$ of the center of NGC 1399 showed a considerably brighter completeness limit by 1–2 mag. The GALEX detections in the output catalogs were then matched with the position of compact Fornax cluster members known from an up-to-date compilation of literature spectroscopic surveys in Fornax, extending to about $V \simeq 22.2$ mag (Kissler-Patig et al. 1999; Mieske et al. 2002, 2004; Dirsch et al. 2004; Bergond et al. 2007; Firth et al. 2007; Richtler et al. 2008; Karick et al. 2008, private communications; see also Tables 1 and 2). There are no compact Fornax cluster members known within $\simeq 2'$ of NGC 1399 (Fig. 1), such that the decline in completeness in this region is irrelevant to this study. The allowed matching radius was 3″, which is about 2 GALEX pixels, or 2/3 of the GALEX PSF FWHM.

All matches on the GALEX images were visually classified in an independent manner by the authors SM and SCR into clear and marginal detections. We retained matches if they were classified as clear detections by both authors. We also accepted matches in a given filter band for which at least one of the authors provided a clear classification, if the source was classified by both authors as a clear detection in the other filter band. We excluded sources from the match list that in higher resolution optical imaging (Mieske et al. 2007) had neighbouring sources within a radius of 4″ not fainter than $V = V_{\rm obj} + 3$ mag. This helped to ensure that the detected UV flux originates in the compact object and not a close neighbour. About 20% of the UV matches were affected by this rejection.

The final sample of visually confirmed *NUV* matches contains 35 objects with $18 < V < 21.4$ mag ($-13.4 < M_V < -10$ mag), while the catalog of *FUV* matches contains 21 objects with $18 < V < 20.8$ mag ($-13.4 < M_V < -10.6$ mag). All of the *FUV* matches are also *NUV* matches. In Tables 1 and 2, the photometric properties of the objects are listed. Figure 1 shows a map of the investigated area and a V, I colour–magnitude diagram which indicates the *FUV* and *NUV* matches and the full literature sample of Fornax compact objects. The photometry was corrected for foreground extinction using the reddening maps of Schlegel et al. (1998). Mainly optically blue GCs are detected in the GALEX images. We attribute this to the fact that the completeness limits of this data set favour the detection of UV bright

[1] http://galex.stsci.edu/GR2/

Table 1. Photometric properties of the 21 compact Fornax cluster members detected in both *NUV* and *FUV* in the GALEX archival images.

ID	RA [2000]	Dec [2000]	V_0 [mag]	$(V-I)_0$	$(NUV-V)_0$	$(FUV-V)_0$	$(FUV-NUV)_0$
UCD3	3:38:54.0	–35:33:33.8	18.03 (0.16)	1.23 (0.12)	3.93 (0.16)	4.42 (0.17)	0.49 (0.06)
UCD6	3:38:05.0	–35:24:09.7	18.89 (0.14)	1.11 (0.11)	3.96 (0.16)	4.61 (0.17)	0.65 (0.12)
UCD27	3:38:10.3	–35:24:06.1	19.66 (0.11)	1.08 (0.06)	3.51 (0.15)	3.21 (0.14)	−0.31 (0.13)
UCD12	3:36:26.7	–35:22:01.6	19.72 (0.03)	1.05 (0.05)	2.89 (0.07)	4.28 (0.14)	1.39 (0.15)
UCD25	3:37:43.6	–35:22:52.0	19.75 (0.06)	0.97 (0.05)	3.26 (0.12)	3.37 (0.11)	0.10 (0.14)
UCDk	3:38:23.7	–35:13:49.4	19.79 (0.06)	0.92 (0.05)	3.46 (0.11)	4.07 (0.12)	0.60 (0.14)
K1011	3:37:24.8	–35:36:10.1	19.88 (0.06)	1.02 (0.05)	4.15 (0.15)	3.72 (0.14)	−0.43 (0.19)
UCD41	3:38:29.0	–35:22:56.6	19.94 (0.07)	1.14 (0.04)	3.58 (0.19)	3.82 (0.13)	0.24 (0.21)
UCDm	3:38:06.5	–35:23:03.8	19.97 (0.06)	0.98 (0.04)	3.77 (0.12)	3.65 (0.12)	−0.13 (0.15)
K1002	3:36:22.2	–35:36:34.6	19.98 (0.06)	0.95 (0.05)	3.20 (0.10)	4.71 (0.17)	1.51 (0.18)
UCD32	3:38:16.7	–35:20:23.3	20.05 (0.06)	0.97 (0.03)	3.60 (0.11)	4.25 (0.24)	0.64 (0.26)
UCD39	3:38:25.5	–35:37:42.6	20.08 (0.07)	1.10 (0.04)	4.57 (0.21)	4.70 (0.18)	0.13 (0.25)
uc218.7	3:38:23.4	–35:39:53.3	20.21 (0.09)	1.43 (0.07)	3.14 (0.15)	3.66 (0.17)	0.52 (0.19)
UCD31	3:38:16.5	–35:26:19.3	20.30 (0.08)	0.93 (0.05)	3.72 (0.16)	4.05 (0.18)	0.33 (0.21)
UCD33	3:38:17.5	–35:33:04.0	20.36 (0.06)	0.97 (0.05)	3.80 (0.15)	4.29 (0.26)	0.48 (0.29)
Y99025	3:38:58.6	–35:26:26.2	20.42 (0.10)	0.94 (0.04)	2.93 (0.15)	3.85 (0.17)	0.92 (0.18)
K1007	3:36:47.6	–35:29:37.3	20.43 (0.07)	0.94 (0.04)	2.95 (0.14)	4.30 (0.21)	1.35 (0.23)
K1000	3:34:51.4	–35:44:02.8	20.44 (0.06)	0.94 (0.05)	3.22 (0.12)	3.89 (0.18)	0.67 (0.20)
UCD38	3:38:25.1	–35:29:25.1	20.49 (0.14)	0.96 (0.12)	3.61 (0.21)	2.93 (0.18)	−0.68 (0.19)
UCD17	3:36:51.7	–35:30:38.9	20.53 (0.08)	1.01 (0.04)	2.40 (0.20)	3.05 (0.16)	0.65 (0.23)
FCOS 0_2032	3:38:30.2	–35:21:31.0	20.82 (0.08)	1.02 (0.08)	3.32 (0.22)	3.23 (0.22)	−0.09 (0.29)

The objects are ordered by increasing V_0 magnitude. The object IDs indicate the following sources: UCDxx = Firth et al. (2007) & Evstigneeva et al. (2008); FCOS xxxxx = Mieske et al. (2002, 2004); Yxxxxx = Richtler et al. (2008); gcxxx and ucxxx = Bergond et al. (2007); Kxxxx = Karick et al. (in preparation, private communications).

Table 2. Photometric properties of the 14 compact Fornax cluster members detected only in the *NUV* GALEX archival images.

ID	RA [2000]	Dec [2000]	V_0 [mag]	$(V-I)_0$	$(NUV-V)_0$
NTT414	3:38:09.7	–35:23:01.3	19.57 (0.17)	0.97 (0.11)	4.12 (0.23)
NTT410	3:38:12.2	–35:24:06.5	19.71 (0.12)	1.18 (0.08)	2.86 (0.25)
UCD20	3:37:27.6	–35:30:12.6	20.04 (0.07)	1.02 (0.04)	3.72 (0.18)
UCD18	3:36:55.5	–35:21:36.0	20.29 (0.04)	0.71 (0.04)	1.29 (0.05)
FCOS 1_0630	3:38:56.1	–35:24:49.0	20.31 (0.08)	1.00 (0.07)	3.19 (0.16)
FCOS 2_2165	3:37:28.2	–35:21:23.0	20.60 (0.08)	0.95 (0.07)	3.44 (0.19)
gc235.7	3:36:12.7	–35:19:11.6	20.64 (0.07)	0.89 (0.03)	2.69 (0.11)
Y7225	3:37:47.2	–35:22:57.4	20.71 (0.10)	0.92 (0.08)	2.82 (0.18)
gc290.6	3:35:42.5	–35:13:52.0	20.92 (0.04)	0.94 (0.02)	1.70 (0.07)
FCOS 1_2089	3:38:48.9	–35:27:43.9	20.97 (0.09)	0.99 (0.08)	3.33 (0.22)
91.041	3:37:56.9	–35:31:50.9	21.12 (0.08)	0.90 (0.05)	2.93 (0.22)
86.112	3:38:41.4	–35:27:41.0	21.29 (0.07)	0.99 (0.05)	2.57 (0.24)
Y1149	3:36:58.0	–35:34:32.2	21.29 (0.06)	0.82 (0.05)	2.17 (0.10)
81.008	3:38:03.0	–35:26:28.3	21.41 (0.09)	0.96 (0.05)	2.55 (0.19)

The objects are ordered by increasing V_0 magnitude. The object IDs indicate the following sources: NTTxxx = Kissler-Patig et al. (1999); UCDxx = Firth et al. (2007) and Evstigneeva et al. (2008); FCOS xxxxx = Mieske et al. (2002, 2004); Yxxxxx = Richtler et al. (2008); gcxxx and ucxxx = Bergond et al. (2007); xx.xxx = Dirsch et al. (2004).

sources in the GC magnitude regime (see next section). In Fig. 1 (right panel), we also indicate data points for GCs in M 31 and M 87 with UV coverage.

3. Results

In Fig. 2 we plot two colour–magnitude diagrams (CMDs) of the *NUV* matches, one of $(NUV-V)$ vs. V, and one of $(FUV-V)$ vs. V. As stated above, all *FUV* matches are also *NUV* matches. We indicate the magnitude dependent colour limits of the data, which biases us towards detecting UV bright objects at fainter optical luminosities (see also Sect. 2). In Fig. 3, we plot colour-diagrams of $(V-I)$ vs. $(NUV-V)$, $(V-I)$ vs. $(FUV-V)$, $(V-I)$ vs. $(FUV-NUV)$, and $(NUV-V)$ vs. $(FUV-NUV)$. In all four plots, we also indicate the GALEX data for GCs in M 31, taken from the compilation of Rey et al. (2007). Furthermore, we show *FUV* data points for the M 87 GCs from the compilation of Sohn et al. (2006). We note that due to the sensitivity limit of our adopted GALEX data, at the distance of Fornax we would be able to detect only two of the M 31 GCs, and none of the M 87 GCs (see Fig. 2).

In the colour–magnitude diagram of $(NUV-V)$ vs. V (Fig. 2, left panel), we find that sources brighter than $M_V \simeq -11.1$ mag exhibit exclusively "red" colours $(NUV-V) \gtrsim 2.7$ mag. Fainter than this luminosity limit, several sources extend to bluer colours $(NUV-V) \simeq 1.0$, indicating a UV excess relative to the brighter objects. We note that $M_V \simeq -11$ mag corresponds to the approximate separation between ordinary GCs and UCDs (Haşegan et al. 2005; Mieske et al. 2006). We can therefore state that seven out of 17 massive Fornax GCs detected in the GALEX images exhibit a UV excess relative to UCDs. Massive Fornax GCs ($M_V > -11.1$ mag) have a mean colour of $(NUV-V) = 2.92 \pm 0.13$ mag, Fornax UCDs ($M_V < -11.1$ mag) have $(NUV-V) = 3.49 \pm 0.17$ mag, while the full sample of

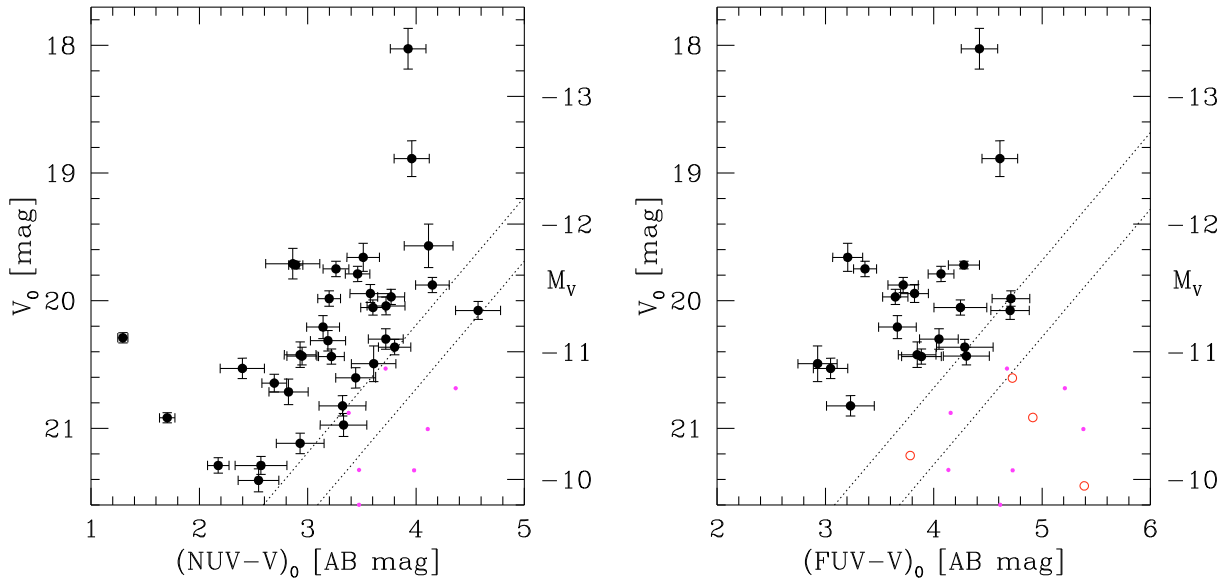

Fig. 2. *Left panel*: $NUV - V$ colour–magnitude diagram of compact objects in the Fornax cluster with matches in the archival GALEX images (see text). Note the possible break at about $M_V \simeq -11.1$ mag. Brighter sources are exclusively red, with $(NUV - V) > 2.7$ mag. The two diagonal dotted lines indicate the 50% and 90% completeness limit of the GALEX detections, as derived from artificial star experiments. Small magenta dots indicate data points for GCs in M 31 (Rey et al. 2007). *Right panel*: $FUV - V$ CMD of compact objects in the Fornax cluster with matches in the archival GALEX images (see text). Small magenta dots indicate data points for GCs in M 31 (Rey et al. 2007). Red circles indicate data points for GCs in M 87 (Sohn et al. 2006).

M 31 GCs has a mean colour of $(NUV - V) = 3.73 \pm 0.07$ mag (see Fig. 3).

Is this relative UV-excess indicative of more extreme horizontal branches in those Fornax GCs? Or is the UV-excess simply due to a far younger age? To address this question, we use a grid of simple stellar population (SSP) models constructed using the Yonsei Evolutionary Population Synthesis (YEPS) code (Park & Lee 1997; Lee et al. 2000; Lee et al. 2005; Yoon et al. 2006, 2008). We note that the models that we use are the latest version of the YEPS models. The version has adopted a new set of HB evolutionary tracks compiled using the identical input physics and equations of state as the Yonsei-Yale (Y^2) MS-RGB evolutionary tracks (Kim et al. 2002), taking into account the α-element enhancement effect. In Rey et al. (2005, 2007) and Kaviraj et al. (2007), the YEPS models were used to investigate the integrated light of GCs in M 31 based on GALEX UV data, and in the Virgo cluster (M 87) based on HST/STIS UV data, respectively. In Lee et al. (2005), the properties of resolved stellar populations in ωCen and NGC 2808 were analysed using the YEPS models (see also Rey et al. 2001, 2004; and Yoon & Lee 2002 for an application to resolved stellar populations in "normal" GCs).

Figure 3 shows that massive Fornax GCs with $(NUV - V) < 2.7$ mag exhibit a UV-excess with respect to the SSP model predictions. There is no combination of age and metallicity that can reproduce these very blue *NUV* colours at the given $(V - I)$: not even isochrones with an enhanced He abundance ($Y = 0.34$ instead of the canonical value $Y = 0.23$) can account for these colours. The UCD data points are more consistent with the model tracks for old ages around 12–14 Gyr. There is a slight UV excess for the optically red UCDs, which can be explained by He enhanced isochrones of old ages.

We now assess whether detecting some massive Fornax GCs with a UV excess indicates that Fornax GCs as a sample have a higher *probability* of having a UV excess than our comparison sample, the M 31 GCs. The two samples are almost disjunct in luminosity (see Fig. 2). We focus on the colour range $(NUV - V) < 2.7$ mag, which is the blue limit of the sample of 87 M 31 GCs with *NUV* detection (Fig. 3), and also corresponds to the blue limit of the UCD colours. From a total of 173 massive GCs with $-11.1 < M_V < -9.9$ mag in the GALEX FoV, only 7 ($4 \pm 1.5\%$) have $(NUV - V) < 2.7$ mag. A Poisson test shows that drawing 0 out of 87 at an underlying assumed probability of $0.04^{+0.015}_{-0.015}$ occurs in $3^{+8}_{-2.1\%}$% of random samplings. We can therefore state that massive Fornax GCs extend to higher *NUV* fluxes than M 31 GCs at the 97% confidence level. We note that none of the 29 UCDs in the GALEX FoV has $(NUV - V) < 2.7$ mag. However, this non-detection is not statistically significant when assuming an underlying probability of $0.04^{+0.015}_{-0.015}$ for a *NUV* excess as deduced from the massive GCs.

In the $(FUV - V)$ vs. $(V - I)$ colour–colour diagram of Fig. 3, a much better age resolution is achieved, but the number of GALEX detections drops to 21, as does the number of M 31 GCs (49 instead of 87 for *NUV*). In this diagram, a UV excess for the 2–3 most metal-rich Fornax UCDs is confirmed, similar to the metal-rich M 87 GCs. Those UCDs show colours best matched with He-enhanced isochrones of old ages 12–14 Gyr. Due to the brighter sensitivity limit of the *FUV* data, only seven massive GCs enter the sample, of which three have UV excess marginally incompatible with He-enhanced isochrones. Given the bias towards detecting UV bright sources and the brighter sensitivity limit in the *FUV* than in the *NUV*, we do not find statistically significant evidence for a different $(FUV - V)$ distribution between Fornax UCDs and massive GCs or M 31 GCs.

The $(FUV - NUV)$ colour–colour diagrams in Fig. 3, especially the diagram $(FUV - NUV)$ vs. $(NUV - V)$, allow the most robust distinction between objects consistent and inconsistent with standard He abundance isochrones. Fornax UCDs with $(FUV - NUV) \lesssim 0.5$ mag show UV colours consistent with enhanced He abundance that cannot be explained by standard He isochrones of 14 Gyr. They also show that at a given colour $(V - I)$ or $(NUV - V)$, UCDs are bluer in $(FUV - NUV)$ than our

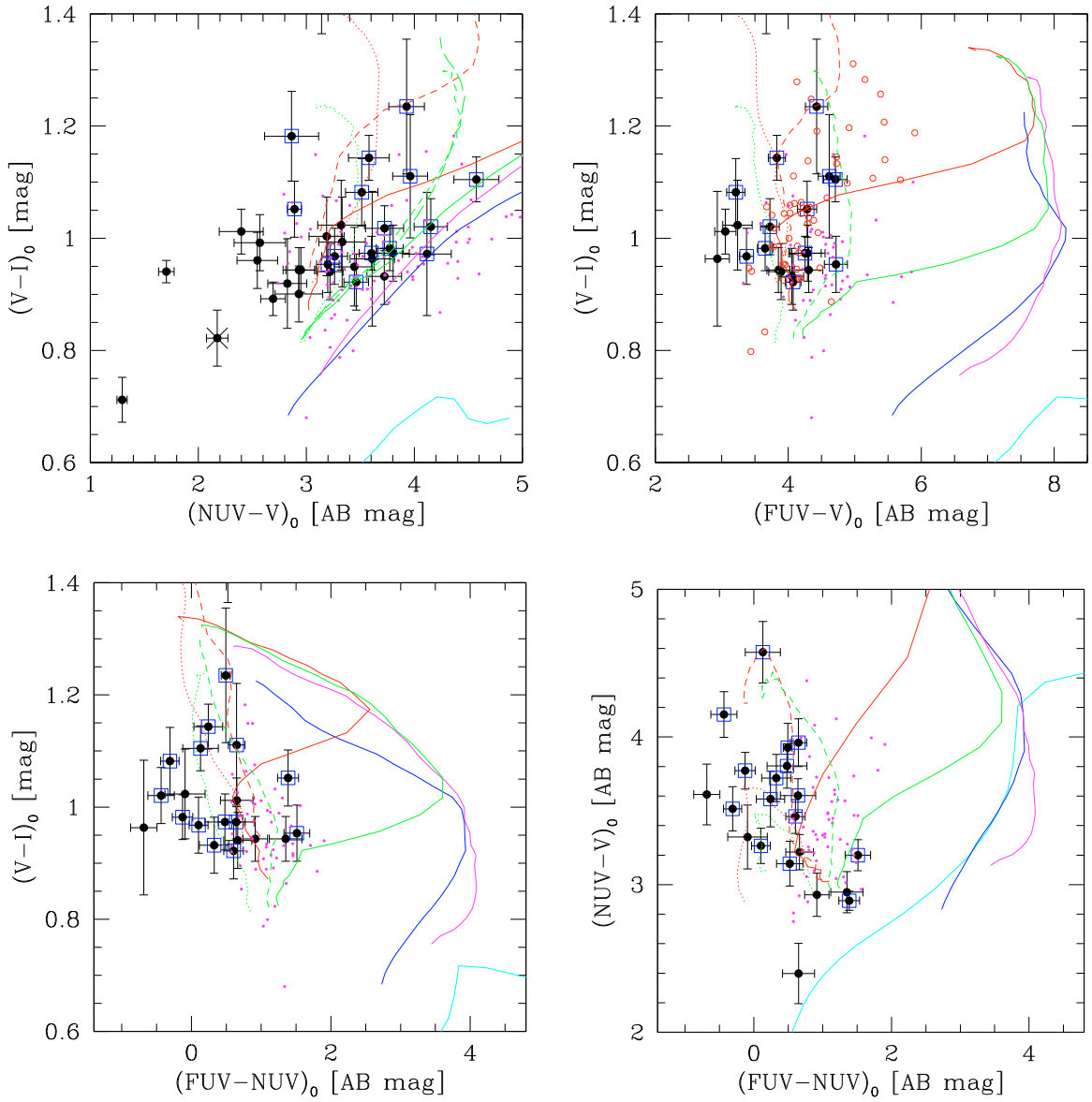

Fig. 3. *Top left panel*: colour–colour diagram of $(NUV - V)$ vs. $(V - I)$ for the objects from Fig. 2. UCDs, i.e. objects with $M_V < -11.1$ mag, are marked by (blue) squares. Overlaid in solid lines are model isochrones from the YEPS models (see text for details) for metallicities between [Fe/H] = −2.5 and 0.5 dex, and assuming [α/Fe] = 0.3 dex. The isochrones correspond to the following ages: 1 Gyr (cyan), 5 Gyr (blue), 9 Gyr (magenta), 12 Gyr (green), 14 Gyr (red). All solid lines assume the standard Helium abundance $Y = 0.23$. The dashed (dotted) lines indicate the 12 and 14 Gyr isochrones for a fraction of 30% (100%) of stars with Helium abundance $Y = 0.34$. The (green) long dashed line shows the 12 Gyr isochrone with a 30% contribution of stars with $Y = 0.40$. There is almost no difference between $Y = 0.34$ and $Y = 0.40$. The source marked by a cross is the only GALEX UV detection that has an X-ray counterpart in the Chandra X-ray images (Scharf et al. 2005). *Top right panel*: colour–colour diagram of $(FUV - V)$ vs. $(V - I)$. Model tracks as in the *left panel*. Red circles indicate data points for GCs in M 87 (Sohn et al. 2006). *Bottom left panel*: colour–colour diagram of $(FUV - NUV)$ vs. $(V - I)$. Model tracks as in the upper two panels. *Bottom right panel*: colour–colour diagram of $(FUV - NUV)$ vs. $(NUV - V)$. Model tracks as in the *upper two panels*.

comparison sample of M 31 GCs. This is the strongest evidence in our data of UCDs as a class harbouring stellar populations with UV excess. We are unable to accurately determine a difference between UCDs and massive Fornax GCs due to the brighter sensitivity limit in the *FUV*, which excludes most of the GCs detected in the *NUV*.

4. Discussion and conclusion

A UV excess in an old stellar population is probably due to EHB stars. As pointed out in Sect. 1, an EHB may be linked to helium-enriched stars (e.g. Ventura et al. 2001; D'Antona et al. 2002). The strong UV excess of the seven massive Fornax GCs beyond the He-enhanced isochrones, especially the *NUV* excess of the three most extreme GCs with $(NUV - V) < 2.4$ mag (see Fig. 3), suggests that in these objects, EHB formation is also driven by other processes. In this context, a plausible explanation may be enhanced mass loss of evolved stars, triggered by high stellar densities (Decressin et al. 2007; Huang & Gies 2006) and/or large binary fractions.

Excess radiation at short wavelengths can in principle also arise from accretion onto a black hole (King et al. 1993), which

can be traced by low-mass X-ray binaries (Jordán et al. 2004). We have cross-checked the positions of all GALEX UV detections with X-ray source detections in the Chandra Fornax Survey data (Scharf et al. 2005 and private communication), the deepest available wide-field X-ray survey of Fornax (50 ks integration with ACIS). The sensitivity of these images is a few 10^{38} erg/s, allowing us to detect the most luminous LMXBs (Jordán et al. 2004). In Fig. 1 (right panel), we indicate the $(V - I)$ optical colours of those compact objects with X-ray matches. At a given magnitude, the X-ray matches in GCs are biased towards red optical colours (see also Jordán et al. 2004), while GALEX UV detections are biased towards blue optical colours. This suggests that in general, the UV- and X-ray-emission of the compact stellar systems are not caused by the same physical processes. However, there is one GALEX UV detection with an X-ray counterpart (Figs. 1 and 3), which happens to be one of the three GCs with the largest UV excess. We cannot therefore exclude that the UV excess in some of the GCs is linked to accretion processes.

We finally note that comparing the probability of UV excess between UCDs and GCs allows to test whether EHBs are more likely associated with present-day deep potential wells (i.e. UCDs) or high stellar densities (i.e. GCs; Dabringhausen et al. 2008; Mieske et al. 2008). One would expect deep potential wells to favour self-enrichment (e.g. Ventura et al. 2001; D'Antona et al. 2002), and high stellar densities to favour mass-loss scenarios (Decressin et al. 2007; Huang & Gies 2006). Such a comparison may therefore help to constrain the efficiency of EHB formation channels, provided that the present-day density and mass of the systems investigated have not experienced significant changes in the past, which would be the case due to core collapse (Noyola & Gebhardt 2006; de Marchi et al. 2007) or tidal stripping (e.g. Lee et al. 2007). To perform this comparison accurately, deeper UV imaging data will be required that allow detection of UV intermediate-bright to faint GCs down to $M_V \simeq -10$ mag ($V \simeq 21.5$ mag at the Fornax distance). In this respect, the results of HST observations in Cycle 15 (GO10901, PI O'Connell) of GCs belonging to NGC 1399 are eagerly anticipated.

Acknowledgements. We are grateful to Caleb Scharf for providing us with the source catalog of the Chandra Fornax survey. We thank the anonymous referee for her/his constructive criticism which helped to streamline the paper. The work of S.-C.R. was supported in part by KOSEF through the Astrophysical Research Center for the Structure and Evolution of the Cosmos (ARCSEC). S.-J.Y. acknowledges support from the Basic Research Program (grant No. R01-2006-000-10716-0) and from the Korea Research Foundation Grant funded by the Korean Government (grant No. KRF-2006-331-C00134).

References

Bedin, L. R., Piotto, G., Anderson, J., et al. 2004, ApJ, 605, L125
Bergond, G., Athanassoula, E., Leon, S., et al. 2007, A&A, 464, L21
Brown, T. M., Sweigart, A. V., Lanz, T., Landsman, W. B., & Hubeny, I. 2001, ApJ, 562, 368
Castellani, M., & Castellani, V. 1993, ApJ, 407, 649
Dabringhausen, J., Hilker, M., & Kroupa, P. 2008, MNRAS, 386, 864
D'Antona, F., Caloi, V., Montalban, J., Ventura, P., & Gratton, R. 2002, A&A, 395, 69
D'Antona, F., Bellazzini, M., Caloi, V., et al. 2005, ApJ, 631, 868
Decressin, T., Meynet, G., Charbonnel, C., Prantzos, N., & Ekstrom, S. 2007, A&A, 464, 1029
D'Cruz, N. L., Dorman, B., Rood, R. T., & O'Connell, R. W. 1996, ApJ, 466, 359
Dieball, A., Knigge, C., Zurek, D. R., et al. 2005, ApJ, 634, 105
Dieball, A., Knigge, C., Zurek, D. R., et al. 2007, ApJ, 670, 379
Dirsch, B., Richtler, T., Geisler, D., et al. 2004, AJ, 127, 2114
Drinkwater, M. J., Gregg, M. D., Hilker, M., et al. 2003, Nature, 423, 519
Evstigneeva, E. A., Drinkwater, M. J., Peng, C. Y., et al. 2008, AJ, 136, 461
Firth, P., Drinkwater, M. J., Evstigneeva, E. A., et al. 2007, MNRAS, 382, 1342
Freedman, W. L., Madore, B. F., Gibson, B. K., et al. 2001, ApJ, 553, 47
Gratton, R., Sneden, C., & Carretta, E. 2004, ARA&A, 42, 385
Haşegan, M., Jordán, A., Côté, P., et al. 2005, ApJ, 627, 203
Huang, W., & Gies, D. R. 2006, ApJ, 648, 591
Jordán, A., Côté, P., Ferrarese, L., et al. 2004, ApJ, 613, 279
Kim, Y.-C., Demarque, P., Yi, S. K., & Alexander, D. R. 2002, ApJS, 143, 499
King, I. R., Stanford, S. A., Albrecht, R., et al. 1993, ApJ, 413, L117
Kissler-Patig, M., Grillmair, C. J., Meylan, G., et al. 1999, AJ, 117, 1206
Kaviraj, S., Sohn, S. T., O'Connell, R. W., et al. 2007, MNRAS, 377, 987
Lee, H.-C., Yoon, S.-J., & Lee, Y.-W. 2000, AJ, 120, 998
Lee, Y.-W., Joo, S.-J., Han, S.-I., et al. 2005, ApJ, 621, L57
Lee, Y.-W., Gim, H. B., & Casetti-Dinescu, D. I. 2007, ApJ, 661, L49
de Marchi, G., Paresce, F., & Pulone, L. 2007, ApJ, 656, L65
Mieske, S., Hilker, M., & Infante, L. 2002, A&A, 383, 832
Mieske, S., Hilker, M., & Infante, L. 2004, A&A, 418, 445
Mieske, S., Hilker, M., Infante, L., & Jordán, A. 2006, AJ, 131, 2442
Mieske, S., Hilker, M., Infante, L., & Mendes de Oliveira, C. 2007, A&A, 463, 503
Mieske, S., Hilker, M., Jordan, A., et al. 2008, A&A, 487, 921
Milone, A. P., Bedin, L. R., Piotto, G., et al. 2008, ApJ, 673, 241
Moehler, S. Dreizler, S., Lanz, T., et al. 2007, A&A, 475, L5
Noyola, E., & Gebhardt, K. 2006, AJ, 132, 447
Park, J.-H., & Lee, Y.-W. 1997, ApJ, 476, 28
Piotto, G., Bedin, L. R., Anderson, J., et al. 2007, ApJ, 661, L53
Rey, S.-C., Yoon, S.-J. Lee, Y.-W., Chaboyer, B., & Sarajedini, A. 2001, AJ, 122, 3219
Rey, S.-C., Lee, Y.-W., Ree, C. H., et al. 2004, AJ, 127, 958
Rey, S.-C., Rich, R. M., Lee, Y.-W., et al. 2005, ApJ, 619, L119
Rey, S.-C., Rich, R. M., Sohn, S. T., et al. 2007, ApJS, 173, 643
Richtler, T., Schubert, Y., Hilker, M., et al. 2008, A&A, 478, L23
Scharf, C. A., Zurek, D. R., & Bureau, M. 2005, ApJ, 633, 154
Sohn, S. T., O'Connell, R. W., Kundu, A., et al. 2006, AJ, 131, 866
Ventura, P., D'Antona, F., Mazzitelli, I., & Gratton, R. 2001, ApJ, 550, L65
Yoon, S.-J., Yi, S. K., & Lee, Y.-W. 2006, Science, 311, 1129
Yoon, S.-J., Joo, S.-J., Ree, Chang, H., et al. 2008, ApJ, 677, 1080